Sun superflaring mechanism from decade-scale magnetic entanglement with Jupiter

Mensur Omerbashich
https://orcid.org/0000-0003-1823-4721, editor@geophysicsjournal.com

Abstract. Sun–Jupiter decade-scale magnetic entanglement emerges from Wilcox Solar Observatory 1975-2021 N–S ≲150 μT mean-field data, as a global response of solar magnetic fields to the magnetar-type evolution of Jupiter ~2001–onward global magnetoactivity discovered recently in the 1–6 month (385.8–64.3 nHz) band of Rieger resonance. At extreme ≲20% field variance, the sudden Jovian deviation is so high it forced solar magnetoactivity devolution into inverse-matching response, at effectively moderate ≲1.5% mean-field variance. Thus as Jupiter magnetoactivity evolved sinusoidally, the Sun began mirror-compensating ~2002 (the epoch of Abbe number drop), reducing its magnetoactivity in decreasingly sinusoidal fashion to solar cycle 24 extreme minimum. For check, 2004-2021 WIND mission data revealed <0.5-var% (<5-dB) calm ≲50 nT interplanetary magnetic field at L1, slightly undulated by the Jupiter evolution impulse, thus excluding solar wind and Sun as impulse sources (confirmed by statistical fidelity waning down Jupiter–L1–Sun diffusion vector spaces, as 10^7–10^3–10^2). Magnetic tangling of stars and hot (<0.1 AU) Jupiters was blamed previously for observed star superflaring 10^2–10^7 times more energetic than the strongest solar flare. Accordingly, the Sun ante-impulse locking is a shock-absorbing mechanism — routine shutter-response to Jupiter recurrent phasing into the flare-brown-dwarf state — with which the Sun enters a grand minimum (sleep mode). As Jupiter intermittently becomes an indirect driver of Earth's climate, the Sun prepares to discharge stored energy as a non-extinction ~10^{32}-erg superflare (currently overdue). The mechanism, in which warm/cold Jupiters too trigger (mild) superflares, possibly defends stars against incoming Jupiters.

Sun–Jupiter magnetic entanglement; solar superflares; pulsar Jupiter; brown dwarfs; Rieger resonance.

1. Introduction

While magnetic field interaction between stars and planets is likely complex, it has been established previously for Sun-like stars and their hot (orbiting the primary star at <0.1 AU) Jupiters that geodynamical properties of a planet are deducible from its detailed magnetic properties (Scharf, 2010). Thus after suspecting Jovian increased magnetoactivity had caused Martian seismicity (Omerbashich, 2021b, 2021c), Omerbashich (2021d) demonstrated magnetar-type ~2002–onward evolution of Jupiter global magnetoactivity and compared this evolution to that of Saturn as the most similar gaseous giant. The Saturn magnetic field has turned out to be tranquil over the same interval, which left an increased Jupiter magnetoactivity as the source of not only seismicity and other geodynamic phenomena but pulsar-beam energy potentially dangerous to Earth as well.

However, magnetic tangling of a Jupiter-like planet and its Sun-like primary via magnetic reconecting perhaps could (pending confirmation from sky surveys) also result in significantly energetic events such as the star *superflaring* — observed emitting up to 10^{38} ergs or 10^2–10^7 times more energy than most energetic solar flares (Rubenstein and Schaefer, 2000), with 10^{33}-erg (non-extinction) events occurring as often as every ~500-600 yr (Maehara et al., 2015). In contrast, while the geological record over the past 2k yr contains no evidence of superflaring (Schaefer et al., 2000), the Sun does seem to set off one 10^{32}-erg such event every ~450 yr (Tsurutani et al., 2003). Since the Earth lacked global aurorae for the past ~500 years as natural companion-events of such a superflare (Rubenstein and Schaefer, 2000), this type of superflaring on the Sun then seems overdue. In addition, superflaring can emerge in a flare star (including subgiant dwarfs) due to magnetic energy stored in the atmosphere and possibly mass transfers (Pettersen, 1989). Kepler mission data confirmed that star flaring is a magnetism side effect by showing that superflares arise on stars with large starspots, but also observed no hot Jupiters around those stars, thus questioning the current models that predict that ~10% of such stars should have hot Jupiters (Maehara et al., 2012). Subsequent TESS mission data from a larger sample of stars (Tu et al., 2020) essentially confirmed the Kepler results. The current models were suspected incorrect also because tidal locking would significantly weaken the magnetic fields of hot Jupiters (Griesmeier et al., 2004).

Therefore, to inspect if the detected Jovian evolution means just the phasing into a flare star (dwarf) itself as surmised by Omerbashich (2021d), or onset of a solar superflare, or both, I here compare the pulsar character of Jupiter to its companion star and examine if the two have magnetically tangled on decadal scales (and thereby entangled). Earlier, Jupiter magnetic field's global dynamics were mapped temporally by the mean-annual effect of that field on the surrounding solar wind (therein used as a proxy) and computed as mean spectra of annual magnetospheric samplings in the 1–6 month (385.8–64.3 nHz) band of wind's Rieger mechanical resonance — a regular yet nonlinear flapping of solar particle ejecta blanketing the ecliptic (Omerbashich, 2021d). Therefore, solar magnetoactivity is examined in the band of Rieger resonance in the present study as well.

2. Data and methodology

To study the evolution of overall solar magnetoactivity, I use the Sun's (both hemispheres) diurnal ≲150 μT Mean Magnetic Field (MMF) data from the Wilcox Solar Observatory (WSO) (Scherrer et al., 1977; ref. Acknowledgments). The background field dominates the MMF in a ~9:1 ratio to other magnetic features including local fields, i.e., sunspots (Bose and Nagaraju, 2018). Since primarily weather conditions controlled the ability to collect data, parts of the record during the summer months were complete, with the remaining portion nearly complete (>90%). Because the telescope operated with a reduced polarization sensitivity due to lens contamination during the 16 December 2016–18 May 2017 interval so that the record did not reflect recalibrated MMF values and only approximate errors are available, possibly making the field samplings nonlinearly noisy, I discard the data from that interval. The analyzed data spanned the WSO record from the start, on 16 May 1975, through 3 August 2021 inclusively.

To temporally map the hyperlow-frequency (<1μHz) dynamics of the solar wind, I spectrally analyze ≲50 nT (≲20 nT most of the time) total-field magnetometer recordings collected between 1995–2021 by the WIND mission (Lepping et al., 1995; ref. Acknowledgments). As in the Jupiter study (Omerbashich, 2021d), the 1–6-month was again the spectral band of choice because it overall reflects the most energetic dynamics (interplanetary dynamics as normalized to the Earth case). After spending most of the initial operational time in a lunar orbit, the spacecraft has been sampling unperturbed IMF in a short fixed orbit at the Lagrangian point L1 continuously since May 2004.

Spectral magnitudes in the present study were computed in both percentages of respective peak's contribution to data variance (var%) and decibels (dB) using the rigorous Gauss–Vaníček (GV) method of spectral analysis (GVSA) by Vaníček (1969, 1971), and plotted against linear background noise levels. GVSA comes integrated with a complete statistical analysis in a scientific software package LSSA that provides periodicity estimates in the strictly least-squares sense, unlike the more popular Lomb-Scargle approximation that underperforms when analyzing noisy and complicated signals, such as those of solar activity (Carbonell et al., 1992; Danilović et al., 2005). Tests of GVSA, showing its superiority, have been performed, e.g., by Taylor (1972) and Omerbashich (2003). Using GVSA has many benefits, including benefits over Fourier methods (Omerbashich, 2021a, 2007, 2006; Press et al., 2007; Pagiatakis, 1999; Wells et al., 1985). By discarding non-recalibrated data in the record, I also take advantage of the blindness to data gaps as a feature exclusive to the least-squares class of spectral analysis techniques.

The same as in the demonstration of increased Jupiter magnetoactivity (Omerbashich, 2021d), change in mean magnetic field activity of the Sun is discerned in the present study by using a spectral method for measuring field dynamics (Omerbashich, 2003, 2007, 2009). In that method, unlike with classically performed comparisons of ratios of Fourier spectral amplitudes to discern field dynamics, average GV variance-spectra over some band of interest, since already directly energy-stratified, represent field dynamics over an epoch of sampling. The same as for Jupiter, the 30–180-days (common) spectral band of solar-wind resonance is used in the present study to represent field magnetoactivity, while one Earth year is again the epoch of choice as before.

3. Results

The solar mean magnetic field responded around ~2002 to the Jovian signal in the same but inverted manner, Fig. 1. In essence, the Sun magnetism compensated by entering into a decreasingly sinusoidal mode, revealing that the two magnetic fields had effectively entangled a very long time ago, so they tangle complexly since. This ante-impulse signature reflects an influx of energy absorbed by an overall and thereby well-tuned oscillatory system. Akin to a car shock absorber, the entanglement represents compensatory dynamics occurring on spatially global and temporally decadal scales. It is only natural then to deduce that this compensation also encompassed the observed lowering of solar activity that soon after ensued in solar cycle 24. However, due to (also natural) insufficient dampening under inherently chaotic overall dynamics of the Sun, incoming energy is never fully absorbed and has to be released somehow to maintain system stability. This state is observed as the ante-impulse decreasingly sinusoidal evolution, e.g., in pulsar 4U 0142+61 (Gonzalez et al., 2010) as it prepared to release surplus magnetic energy in the form of a superburst. The same then can be expected of the Sun, so its response mechanism to Jupiter pulsation phase is at the same time the Sun's superflaring mechanism. Note that there are many other examples of decreasingly sinusoidal (increasingly pulsating) mode of energy diffusion, e.g., a most common such occurrence is in the preparation stage of explosive discharge imminent in compressively overloaded closed physical systems.

As seen in more detail in Fig. 2, the Sun has compensated for the Jupiter impulse with the subsequent solar cycle (24) that began in 2009 (by 2012 fully), including the lowering of solar activity. Thus the Sun–Jupiter decade-scale magnetic entanglement provides a physical explanation for the observed record-low solar activity of the last decade, starting with the 2014 maximum of the cycle 24 and the preceding minimum of 2009 (Fig. 2-a), both being among the weakest on proxy record (Basu, 2013) and weakest on instrumented record. In a study of the long-term evolution of solar activity, a proxy dataset spanning the last 11.5 kyr has shown that a stochastic (therefore not necessarily internal) process drives the recurrence of solar grand minima/maxima. The same study also showed that these events cluster in time, with long event-free periods between the clusters — indicating that the Sun dynamo is controlled by processes related to accumulation and release of energy (Usoskin et al., 2007). That result supports the situation in which Jupiter phases in and out of its active states, every time pending sufficient accumulation of magnetic–rotational energy to the point of criticality. Then the subsequent Jupiter–Sun magnetic reconnecting, occurring in a situation of increased Jovian magnetoactivity, makes the Sun compensate for reactivated pulsar Jupiter by lowering solar activity to the point of a grand minimum.

Year	var%	dB	Year	var%	dB	Year	var%	dB
1975	0.9	-25.5	1991	0.5	-26.5	2007	0.4	-26.2
1976	0.8	-23.6	1992	1.6	-19.7	2008	0.4	-28.6
1977	1.0	-23.7	1993	0.5	-26.5	2009	0.5	-25.3
1978	0.9	-23.8	1994	0.8	-24.7	2010	0.9	-23.9
1979	0.6	-25.3	1995	0.7	-24.0	2011	0.8	-23.4
1980	0.8	-22.1	1996	1.0	-21.3	2012	0.6	-24.9
1981	0.9	-21.9	1997	1.7	-20.7	2013	1.0	-23.5
1982	0.7	-28.4	1998	0.4	-25.8	2014	1.3	-21.5
1983	0.4	-26.8	1999	0.7	-24.8	2015	0.6	-24.1
1984	0.5	-24.7	2000	0.6	-24.6	2016	0.6	-24.3
1985	1.3	-21.7	2001	1.2	-21.8	2017	1.5	-20.0
1986	0.5	-25.1	2002	0.9	-22.7	2018	0.5	-25.3
1987	1.2	-23.9	2003	0.7	-24.2	2019	0.7	-25.2
1988	1.7	-21.4	2004	0.5	-26.1	2020	1.8	-19.3
1989	2.2	-21.9	2005	1.0	-21.1	2021	1.8	-22.5
1990	2.4	-18.6	2006	0.7	-24.2			

Table 1. Spectral values for the Wilcox Solar Observatory solar mean magnetic field, Fig. 1.

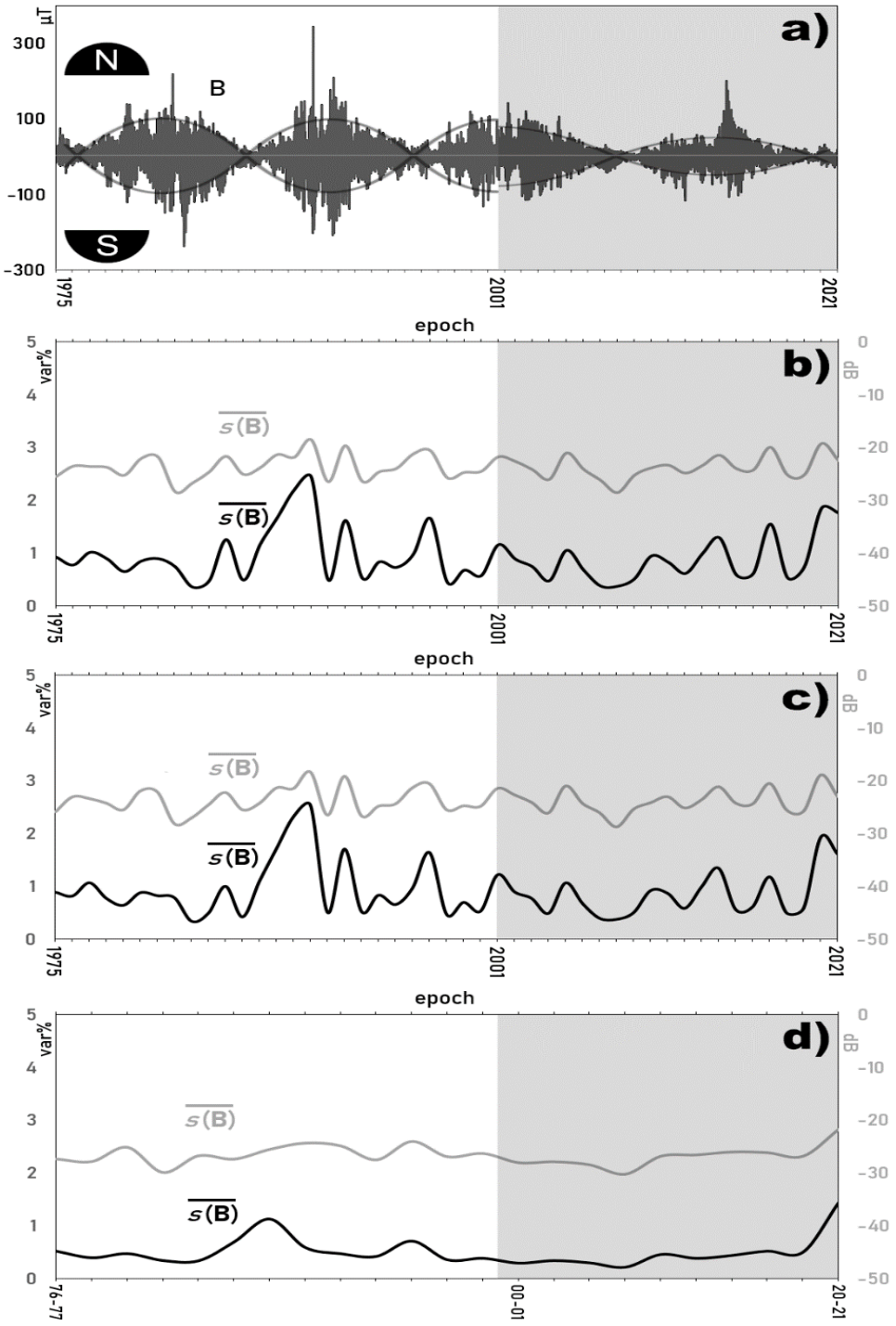

Figure 1. Sun overall magnetoactivity since 1975. Panel a: Wilcox Solar Observatory mean magnetic field (MMF) diurnal variations (of B) in μT, depicting sudden and controlled sunwide dampening of field oscillations from ~2002 on, which coincided in time with the onset of ~2001–onward magnetar-type evolution of Jupiter global magnetoactivity (Omerbashich, 2021d). Panel b: Sun overall magnetoactivity evolution as a change of mean-annual Gauss-Vaníček (GV) spectral magnitude in var% (solid line) and dB (gray) of field variations from panel (a), 30–180-days (385.8–64.3 nHz) band. The depicted solar overall magnetoactivity shows the Sun's response to a globally forced (extrasolar) event since ~2002, in the form of an ante-signal to the Jovian such evolution, revealing that Sun had to compensate for the sudden energy surplus by lowering its activity, to a record minimum already in solar cycle 24. Panels c-d: an examination of signal strength and clarity, by moving the band's lower end: (a) by shortening to 30–140-days to exclude the Rieger period and leave Rieger harmonics only, and (d) by expanding to 30–300-days (and data then to 2-yr bins) to include the first mid-term Rieger reflection (Bai, 2003). The shortening affected signal clarity, so the ante-impulse can be recovered if considering the whole Rieger resonance only. The expansion has affected the signal by virtually extinguishing it, confirming that only the Rieger resonance band enables recovery of the ante-impulse. Thus the Rieger band is a natural band of the overall solar activity, with the Rieger period as the fundamental note. Gray boxes: time interval of the Jupiter evolution impulse and Sun ante-impulse. For the data source for panel (a), see Acknowledgments. Data for panels (a)–(c) are in Table 1.

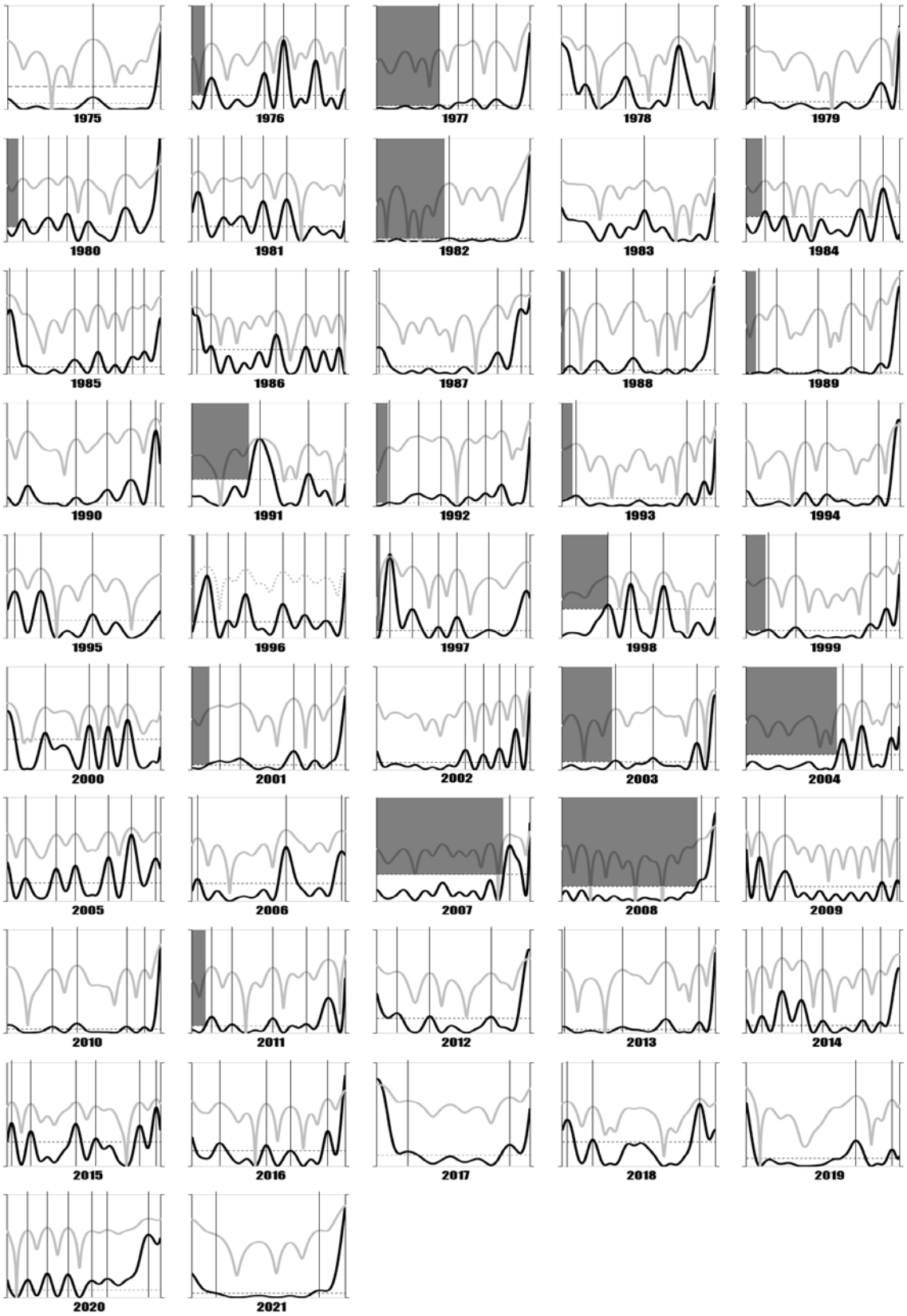

Figure 2. A blind-plots stack of MMF's GV spectra in var% (dark lines) and dB (light lines), showing mixed-rate (highly turbulent) anisotropic peak splitting under Sun magnetoactivity since 1975. The overwhelming influence of increased Jupiter magnetoactivity past ~2002 is seen as the extinguished lowest frequencies, i.e., the most energetic mean-field dynamics (gray boxes). In the absence of turbulent fields, the Jupiter case revealed no systematic (prolonged) extinguishing in the lowest frequencies; see Fig. 1–right panel by Omerbashich (2021d). The Sun compensated the Jupiter impulse with the solar cycle 24 in 2009, fully by 2012, including the lowering of solar activity. Note that the 1982 case was due to a solar minimum. Amplitudes not to scale. Short-dashed line marks confidence at 67% and practically coincides with the abscissa in most panels, with the 99% level always nearby (shown long-dashed on the 1975 plot for illustration). See Supplement for data.

As To statistically verify that the solar activity drop as seen on Fig. 1-b indeed was both sinusoidal and sudden, and to discern its timing, I compute the Abbe number, $\mathcal{A}$, which quantifies signal smoothness (or roughness) by comparing mean square successive differences of a time series x_i of n values and the mean $\bar{x}$, against variance (von Neumann, 1941, 1942):

$$\mathcal{A} = \frac{n}{2(n-1)} \frac{\sum_{i=1}^{n-1}(x_{i+1} - x_i)^2}{\sum_{i=1}^{n}(x_i - \bar{x})^2}. \quad (1)$$

The Abbe number decreases as signal smoothness increases. As seen from Fig. 3, this verification turned out positive for both of the above-implied spatiotemporal manners in which the Sun magnetoactivity devolved from 1975–2021.

To physically verify the directionality of Jupiter–L1–Sun impulse propagation down the respective vector spaces, I compute the IMF magnetoactivity at the Lagrangian point L1, midway between the Sun and the Earth. As it turned out, the IMF at L1 has also responded to the signal past 2004, albeit only slightly so, Fig. 4. To statistically verify the result, for each estimated spectral peak, its fidelity values were used, and then those statistics from the three locations (Jupiter, Sun, L1) were compared; Fig. 5.

As seen from Fig. 5, in the Jupiter case (Omerbashich, 2021d), statistical fidelity on spectral peaks estimates stayed well within a very high ($\Phi \gg 12$) range, of 10^7–10^5 going from lowest- to highest-frequency spectral peaks, respectively (Omerbashich, 2021d), where $\Phi > 12$ is indicative of a physical process (Omerbashich, 2006). Thus, the imprint of Rieger-resonating solar-wind dynamics onto the Jovian magnetopause and below was both total and incessant for all practical purposes. Note that the fidelity in Saturn spectra (not shown) was over half an order of magnitude below that in Jupiter spectra, in the $3.7 \cdot 10^6$–10^5 range, but still higher than for either the Sun or the IMF at L1 (both nearly the same distance from Jupiter), reflecting an added influence of Jovian magnetotail on Saturn magnetoactivity and vigor of Rieger resonance near Saturn.

In the Sun case (WSO data), fidelity was between 44–14 on the lowest and 5–1 on the highest frequencies, indicating that, within the band of interest, the Sun had emitted energy only in the lowest (strongest-energy) frequencies, i.e., just about responded to an external process as the Sun was almost out of reach of the Jupiter impulse while the higher frequencies were sporadic and therefore uncharacteristic, Fig. 2. Therefore the imprint of the Jupiter impulse onto the solar magnetosphere was incomplete and incessant.

In the IMF case (WIND data), fidelity was between 1100–360 on the lowest and 53–30 on the shortest frequencies, indicating that IMF at L1 was well within reach of the Jupiter very-long-period (decade-scale-) magnetic impulse to respond to it magnetically as well, i.e., to allow it to slightly moderate IMF amplitudes, Fig. 4.

Thus, statistical fidelity of the computed frequency spectra is seen as naturally (upstream the solar wind) diminishing down the impulse propagation vector spaces Jupiter–L1–Sun, as 10^7–10^3–10^2 respectively, confirming that the impulse is genuine while corroborating impulse general direction, as well as the physical interpretation of the result.

Year	var%	dB	Year	var%	dB	Year	var%	dB
1975	0.3	-26.4	1984	0.7	-24.7	1993	0.4	-25.9
1976	0.3	-26.6	1985	0.4	-25.5	1994	0.9	-22.7
1977	0.3	-28.1	1986	0.4	-26.6	1995	0.4	-25.4
1978	0.2	-28.9	1987	0.2	-28.9	1996	0.2	-30.1
1979	0.3	-28.6	1988	0.1	-30.4	1997	0.2	-31.2
1980	0.3	-27.3	1989	0.3	-26.6	1998	0.2	-29.3
1981	0.4	-26.8	1990	0.6	-24.9	1999	0.3	-27.8
1982	0.6	-24.9	1991	0.5	-27.2	2000	0.3	-27.7
1983	0.4	-26.7	1992	0.5	-26.3	2001	0.4	-26.6

Table 2. Spectral values for WIND mission interplanetary magnetic field data, Fig. 4.

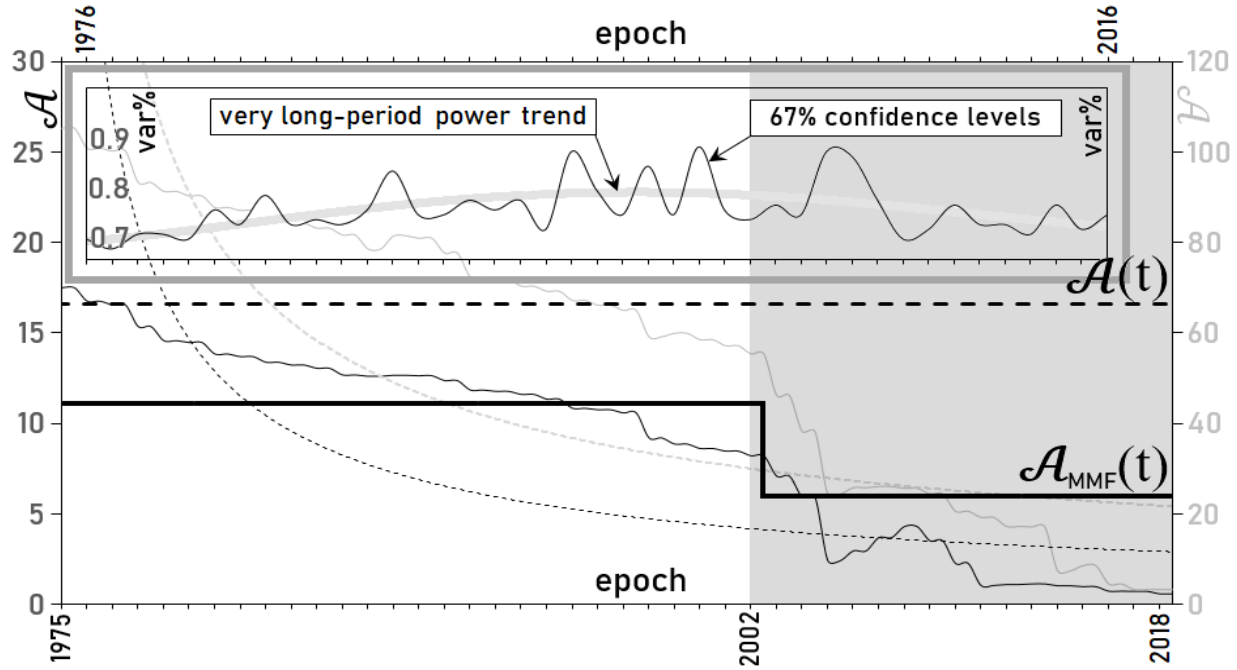

Figure 3. Plots of scaled Abbe numbers, $\mathcal{A}$, for the time series from Table 1, of GV epoch-mean spectra of 1975–2021 Wilcox Solar Observatory mean magnetic field diurnal data. Drop epoch determined by shifting (shortening) the time series one epoch at the time, on through 2019: for mean variance-spectra — thin dark line with power trend as dark-dotted; for mean power-spectra — thin light line with power trend as light-dotted. Note that downward linear trend (not plotted) in the $\mathcal{A}$ number from shifted time series is due to data shortening, and therefore not genuine (see callout for the real trend). Based on the drop epoch thus determined as ~2002, $\mathcal{A}_{MMF}$(t) numbers were computed for pre-drop (1975–2002 conclusive) and post-drop (2003–2021) portions of the time series, Eqn. (1) — thick step-line with the $\mathcal{A}$(t) of the total time-series as thick dashed. Comparison between the two thick lines and between the steps confirms that the drop was sudden and of ~5% mean-field variance, so the post-drop portion of the time series describes a relatively most smooth function, here sinusoidal. Note that the final plunge in $\mathcal{A}$ occurred in 2009, i.e., at the onset of solar cycle 24, further contributing to regular activity decrease. Gray box: time interval of the Sun ante-impulse to the Jupiter evolution impulse, Fig. 1-b. Callout: plot of epochal 67% confidence levels from 1976–2016 (end-epochs with ≳1/2-yr data gaps omitted) in var%, showing the real (very long period-) power trend in the Sun internal energy dynamics as the thick gray curve, thanks to the GV linear background noise levels and thus variance-spectra directly measuring system energy levels (Omerbashich, 2003, 2007, 2009). The trend probably extends to centennial scales and reflects known global solar variations down to millennial scales, such as the Hallstatt cycle, of ~2400 yr, at which solar grand minima and maxima cluster (Usoskin et al., 2016).

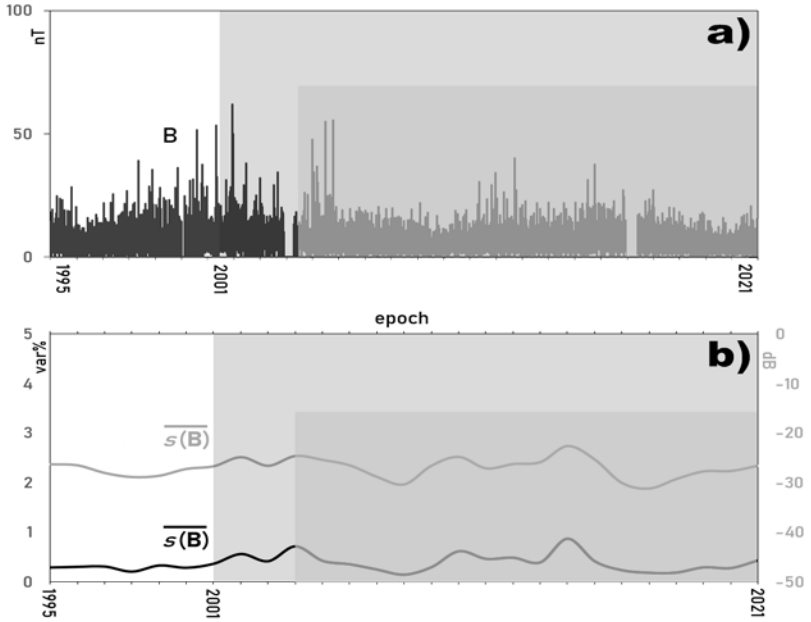

Figure 4. Panel a: 1995-2021 unperturbed ≲50 nT (<20 nT most of the time) IMF data from the WIND mission at the Lagrangian point L1 (in L1-fixed orbit continuously since 2004). Panel b: GV spectra (as for Fig. 1-b–d) revealed a <0.5-var% (<5-dB) calm interplanetary magnetic field (IMF), as effectively slightly undulated by the Jupiter evolution impulse (observed visually since data size was insufficient for relative Abbe number computations as those in Fig. 3). This result excludes both the IMF and Sun as impulse sources: IMF — because L1 is closer to the Sun than Jupiter is yet considerably less affected by the impulse, and the Sun — because it is the source of the solar wind, which ought then to preserve (or, shape the IMF at L1 into) the signature of such Sun-originating impulses if any. Lighter gray boxes: time interval of the Jupiter evolution impulse and Sun ante-impulse. Darker gray boxes: time interval of continuous coverage of IMF at L1 by WIND.

Since the Jupiter magnetic field is rotational in character, the Jovian magnetosphere and any associated pulsar energy emissions are moderated largely by incoming mass transfers (from solar wind primarily). Besides, variance spectra as such (naturally) are energy stratified. This situation justified taking the IMF variance, as represented by the Rieger resonance variance-spectra and its energy band, proportionate to the Jovian magnetic field variance. This logical extension forms the nature of the magnetic field's signature as impressed onto the solar wind — used then as a proxy of global magnetoactivity. On the other hand, since the character of Sun overall magnetic activity remains extremely complex to decipher and thus hard to model or predict, the uncertainty in relating mean-field variance to a narrowed-field-variance as described spectrally in the band of interest is non-obvious, but also of no concern here given the relatively lower effective spectral response of the Sun. As in the Jupiter study, while the 99%-significance level in all cases was very close to the 67% level, the latter was considered sufficient for validating widely reported physical period ensembles such as the Rieger periodicities. Such reasoning was justified subsequently by those levels revealing a centennial trend, Fig. 3-callout.

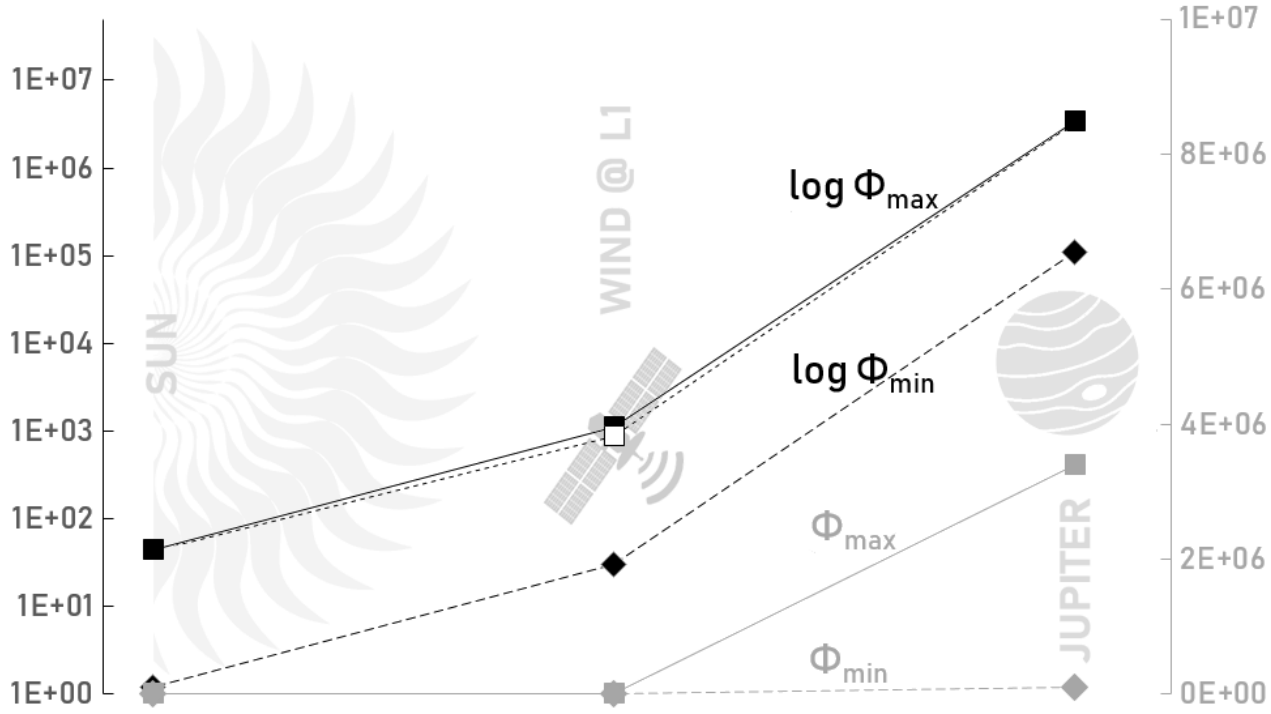

Figure 5. Plot of spatially changing maximum values (Φ_{max} — square markers) and minimum values (Φ_{min} — rhombus markers) of statistical fidelity, Φ, for frequency spectra of Rieger resonance 2000–2021. Left column — at the Sun (Wilcox Solar Observatory telescope MMF data); Middle — at the Lagrangian point L1 in the interplanetary magnetic field (IMF) midway between the Earth and the Sun (WIND mission data since 2004 – white marker and dotted lines); Right — at Jupiter (Galileo, Cassini, Juno missions data). The drop reflects the natural dissipation of Jupiter magnetic energy so that only logarithmic representation (black lines and markers) maintains the range, while numerical representation (gray lines and markers) does not. While IMF strength varies greatly and is independent of the distance from the Sun, the depicted exponential (naturally upstream the solar wind) waning of fidelity down the impulse diffusion vector space Jupiter–L1–Sun, as 10^7–10^3–10^2 respectively, highlights Jupiter as the source of the emission and thus eliminates both the solar wind and the Sun as impulse sources.

4. Discussion

Rieger resonance arises due to the Sun's internal processes or physics of planetary constellations acting as natural obstacles and consists of the P_{Rg} = ~154-day driver (Rieger et al., 1984) called Rieger period, and its 5/6 P_{Rg}, 2/3 P_{Rg}, 1/2 P_{Rg}, 1/3 P_{Rg}, 1/4 P_{Rg}. 1/5 P_{Rg} harmonics or ~128, ~102, ~78, ~51, ~38, ~30-day periods called Rieger-type periodicities (Dimitropoulou et al., 2008). A periodically forced damped nonlinear oscillator that exhibits periodic and chaotic behavior can model this resonance (Bai and Cliver, 1990). Subsequently, P_{Rg} resonance was confirmed in the interplanetary magnetic field (IMF), including IMF near the Earth (Cane et al., 1998) and most heliophysics data types such as solar flares, photospheric magnetic flux, group sunspot numbers, and proton speed, and in different ranges depending on the data, location, epoch, and methodology, as 155–160 days, 160–165 days, 175–188 days, and 180–190 days (Gurgenashvili et al., 2017). Thus while Rieger resonance occurs in various subbands, they share a band — of 30–180-days. Historically, the Rieger period has decreased until the middle of the last century and then began to increase again towards the end of the century, opposite to the activity magnitude trend (Zaqarashvili et al., 2021). Likewise, Rieger-type periodicities also correlate with solar cycle strength and are shorter during solar cycles with higher magnetic activity (Gurgenashvili et al., 2016). This situation implies that Rieger resonance originates in the Sun engine. However, possible upstream waves in the solar wind from termination shock on the order of a few days and longer were implied from Voyager 2 mission samplings of the solar wind on entry into the interstellar space, allowing for the classical explanation according to which mechanical resonance arises in the solar wind due to waves encountering physical obstacles along propagation paths.

Since ~2001, Jupiter decade-scale global magnetoactivity evolution in the band of Rieger resonance took an increasingly sinusoidal form seen in magnetar 4U 0142+61 (Omerbashich, 2021d). The mode of system tiredness in which a system dissipates energy in an increasingly sinusoidal manner is in astrophysics found not only in magnetars but in other bodies as well; for example, superhumps or superoutbursts (long outbursts) are seen in dwarf novae when a non-sinusoidal pulse shape becomes increasingly sinusoidal as the amplitude declines (Kuznetsova et al., 1999). In geology, the above release regime is part of metasomatic metamorphism — a chemical transformation of rock due to fluid-induced reaction, e.g., Aulbach et al. (2018). Thus, as cross-scale and cross-discipline, this type of system energy dissipation could be more common in nature than previously thought.

To verify the directionality of the Jupiter pulsation signal necessitated looking into the Sun magnetoactivity in the same spectral band (or Rieger resonance) and over the same time interval. Because it lacks large-scale geometries and instead consists of complex ~$10–10^4$-km large and up to ~$0.1 \cdot R_{\odot}$ high structures, solar magnetosphere commonly is pluralized as 'magnetic fields' — making computation of any response of the Sun in the band of interest piece-wise (field-by-field) difficult, so that the MMF was studied instead. While averaging a field does smooth out many intricacies, some still endure in the MMF even though the background field is dominant (Bose and Nagaraju, 2018). That problem was in the present study further addressed and resolved by applying a robust, rigorous, and gaps-insensitive spectral analysis method and approaches.

Sun-like stars with planetary systems expectedly erupt with superflares (Schaefer et al., 2000). While Jupiter-like gaseous giants in close orbits about Sun-like stars could theoretically cause such events, Jupiter appears to be too remote from the Sun to cause a solar superflare via magnetic tangling under reconnecting (Rubenstein and Schaefer, 2000). However, since the physics of such magnetic reconnections largely remains unknown (*ibid*.), a Jupiter-like gaseous giant with its own flaring mechanism (regardless if capable of flaring or not), especially if that mechanism were purely magnetic and rotational like Jupiter's, could also entangle its primary star's magnetic field on decadal scales without causing star rotational variations or extinction-level superflares. This scenario is particularly plausible as the geological record does not contain a link between mass extinctions and solar superflares (*ibid*.).

A conventional but *ad hoc* criterion for regarding a planet to be a brown dwarf is that the planetary mass must exceed 13.6 $M_{Jupiter}$ — while another criterion, defended by an important fraction of the astronomical community, is based on the origins of the object's formation instead (Chauvin et al., 2005). While the difference between a high-mass gaseous planet like Jupiter and a low-mass brown dwarf is still a matter of debate, it is rather unfortunate that neither of the above most vocal schools of thought (scale-based and

internal-physics-based criteria v. way-of-formation criteria) advocates external physics, i.e., current activity or lack of it, as the criterion.

Just as gaseous giant planets often are termed *failed stars* for their inability to sufficiently amass and ignite a core early on in their history, Jupiter too is termed *failed brown dwarf* (Fukuhara, 2020). However, in reality, those objects have not failed in cases where their physical or chemical properties amount to star-like global activity sufficient to act on active (fusing) stars. As the present and to it preceding Jupiter studies have shown, low-mass magnetic stars like our Sun are affected globally by gaseous magnetic giants like Jupiter that are not orbiting as nearby as hot Jupiters. Based on its activity type and extent rather than purely scale-based (therefore arbitrary) conventional criteria like mass or distance from the primary star, Jupiter meets natural criteria to be re-classified as a pulsar — it behaves under its own rotation like any magnetar pulsar and affects its primary star just as a dwarf star in binary solar systems does. Importantly, planetary-mass brown dwarfs have been observed (Luhman et al., 2005).

While it is difficult to locate its origin in time, it is easy to see through extrapolation — especially since the solar and thus the IMF strengths tended to increase freely after the last (Maunder) grand minimum (Lockwood et al., 1999) — that the Sun–Jupiter decade-scale magnetic entanglement had already commenced during one of the previous grand minima. Such extrapolation paints a picture of an otherwise chaotic star that, if unchecked, could become far more dangerous than is presently the case, where magnetar dwarf Jupiter keeps it in check. Thus solar grand minima act as the Sun shutter-response to pulsar Jupiter recurring active phase, routinely making Jupiter an indirect but significant Earth climate driver, as deduced previously from orbital geometry, e.g., by Niroma (2009). In that sense, the well-known Schwabe–Wolf cycle of sunspots recurrence itself, of ~11 yr in duration, is the sunwide enforced Jupiter orbital period, of ~11.86 yr, where highly turbulent and mutually interacting solar magnetic fields result in that cycle's quasiperiodic nature.

Besides, there can be little doubt that the Sun had activated this protective mechanism a long before humans began observing solar sunspot (local magnetic) activity — probably while Jupiter was still migrating to its current position inward (for a review of planetary migration models, see, e.g., Raymond and Morbidelli, 2022). As a defense mechanism of Sun-like stars, and therefore a defense mechanism of many normal stars too, the decade-scale magnetic entanglement could explain observations from the Kepler mission according to which only ~1% of gaseous giants orbiting Sun-like stars are hot Jupiters, whereas ~99% are warm/cold — orbiting at distances >0.5 AU like Jupiter (at ~4–6 AU).

Given the global and decadal nature of the superflare mechanism and its recurrence rate along century or longer scales, one can speculate that this "star shield from incoming fire" explains why only <1% of all Jupiters are hot Jupiters. Namely, besides just lowering solar activity, the mechanism perhaps also keeps Jupiter a safe distance by hindering its abilities to attain a corrected orbit. This blocking could occur via atmospheric depletion (Lalitha et al., 2018) or Jupiter scattering more mass during grand minima (due to lower production of the solar wind) than it accrues (Adams, 2011), or by preventing Jupiter clenching onto the Sun magnetism, or in a combination of those. Both of these ways (gravitational and electromagnetic), if unchecked, enable Jupiter to climb its distance to the Sun. If true, this solar last line of defense against migrating-in Jupiters is a universal stellar mechanism for preventing gaseous giants from ever leeching in, i.e., becoming hot Jupiters via penetrating primary star's defenses and assuming a <0.1 AU orbit when the star's and the existence of its planetary system could become jeopardized. In turn, the forever-banished Jupiter, in most cases deprived of proximity to its binary companion, as such then lacks any potential for firing extinction-level superflares itself. On the other hand, both solar and Jovian unevenly explosive bursts still can be expected but also constrained by a mutual balance.

5. Conclusions

Even though it hosts several gaseous giants in its heliosphere, the Sun lacks extinction-level superflaring ability observed throughout the universe, largely thanks to its protective shutter-mechanism, akin to a car shock absorber but with the appearance of a camera lens cover, which signals the Sun to lower magnetic activity. Thus as soon as it recognizes the (astrophysical) signature of a sudden energy influx such as a superhump or here the Jupiter's magnetar-type evolution impulse (regardless if Jupiter had in the meantime since the last time it locked magnetically with the Sun developed the actual superflaring potential or not), the Sun enters into a "sleep mode" (grand minimum). Each dramatic reduction in (magnetic) activity eventually must end in an energetic burst of the suppressed energy — a superflare. However, also thanks to that mechanism, the Sun effectively prevents any extinction-level such superflaring that could ensue if the Jupiter magnetic impact were to go unchecked.

While the Jupiter orbiting distance and the absence of superflare-related extinctions from 0–2-kyr BP geological record make cataclysmic solar and Jovian superflares less likely, the current global locking of the two most powerful magnetic fields in the solar system reflects Jupiter again re-phasing into the flare-brown-dwarf state and our solar system into distantly–binary. Therefore, the ongoing episode of Sun-Jupiter magnetic entanglement could represent the onset of a 10^{32}-erg (non-extinction) superflare, which appears to be overdue.

Astrophysical models of star superflaring need to account for the here revealed ability of pulsar Jupiters at distances beyond 0.1 AU to trigger mild (non-extinction) superflares.

Acknowledgments and Data & Code Statements

The Wilcox Solar Observatory data source was http://wso.stanford.edu/#MeanField. NASA's Space Physics Data Facility and Dr. Adam Szabo (Goddard Space Flight Center) are providers of the WIND mission data: https://cdaweb.gsfc.nasa.gov/pub/data/wind/mfi/ascii/. The least-squares spectral analysis scientific software LSSA, based on the rigorous method by Vaníček (1969, 1971), was used to compute spectra. Dr. Spiros Pagiatakis (York University) provided LSSA v.5.0, which is now available as an open-source version from http://www2.unb.ca/gge/Research/GRL/LSSA/sourceCode.html. All data analyzed in this study are enclosed in a Supplement accompanying this manuscript.

Declarations

The author reports no competing interests.

References

Adams, F.C. (2011) Magnetically controlled outflows from hot Jupiters. *Astrophys. J.* 730:27. DOI: https://doi.org/10.1088/0004-637X/730/1/27

Aulbach, S., Heaman, L.M., Stachel, T. (2018) *The Diamondiferous Mantle Root Beneath the Central Slave Craton*. Geoscience and Exploration of the Argyle, Bunder, Diavik, and Murowa Diamond Deposits. ISBN 9781629496399. DOI: https://doi.org/10.5382/SP.20.15

Bai, T. (2003) Hot Spots for Solar Flares Persisting for Decades: Longitude Distributions of Flares of Cycles 19-23. *Astrophys. J.* 585:1114-1123. DOI: https://dx.doi.org/10.1086/346152

Bai T. and Cliver E. W. (1990) A 154 day periodicity in the occurrence rate of proton flares. *Astrophys. J.* 363:299-309. DOI: https://doi.org/10.1086/169342

Basu, S. (2013) The peculiar solar cycle 24 — where do we stand? *J. Phys.* 440:012001. DOI: https://doi.org/10.1088/1742-6596/440/1/012001

Bose, S., Nagaraju, K. (2018) On the variability of the Solar Mean Magnetic Field: contributions from various magnetic features on the surface of the Sun. *Astrophys. J.* 862:35. DOI: https://doi.org/10.3847/1538-4357/aaccf1

Cane, H.V., Richardson, I.G., von Rosenvinge, T.T. (1998) Interplanetary magnetic field periodicity of ~153 days. *Geophys. Res. Lett.* 25(24):4437-4440. DOI: https://doi.org/10.1029/1998GL900208

Carbonell, M., Oliver, R., Ballester, J.L. (1992) Power spectra of gapped time series: a comparison of several methods. *Astron. & Astrophys.* 264:350-360. BIB: https://ui.adsabs.harvard.edu/#abs/1992A&A...264..350C

Chauvin, G., Lagrange, A.-M., Zuckerman, B., Dumas, C., Mouillet, D., Song, I., Beuzit, J.-L., Lowrance, P., Bessell, M.S. (2005) A companion to AB Pic at the planet/brown dwarf boundary. *Astron. Astrophys.* 438(3):L29-L32. DOI: https://doi.org/10.1051/0004-6361:200500111

Danilović, S., Vince, I., Vitas, N., Jovanović, P. (2005) Time series analysis of long term full disk observations of the Mn I 539.4 nm solar line. *Serb. Astron. J.* 170:79-88. DOI: https://doi.org/10.2298/SAJ0570079D

Dowden, R.L. (1968) A Jupiter Model of Pulsars. *Publications of the Astronomical Society of Australia* 1(4):159–159. DOI: https://doi.org/10.1017/s132335800001122x

Fukuhara, M. (2020) Possible nuclear fusion of deuteron in the cores of Earth, Jupiter, Saturn, and brown dwarfs. *AIP Advances* 10:035126. DOI: https://doi.org/10.1063/1.5108922

Gonzalez, M.E., Dib, R., Kaspi, V.M., Woods, P.M., Tam, C.R., Gavriil, F.P. (2010) Long-term X-ray changes in the emission from the anomalous X-ray pulsar 4U 0142+61. *Astrophys. J.* 716:1345–1355. DOI: https://dx.doi.org/10.1088/0004-637X/716/2/1345

Griesmeier, J.-M., Stadelmann, A., Penz, T., Lammer, H., Selsis, F., Ribas, I., Guinan, E.F., Motschmann, U., Biernat, H.K., Weiss, W.W. (2004) The effect of tidal locking on the magnetospheric and atmospheric evolution of "Hot Jupiters". *Astron. Astrophys.* 425(2):753-762. DOI: https://doi.org/10.1051/0004-6361:2003568

Gurgenashvili, E., Zaqarashvili, T.V., Kukhianidze, V., Oliver, R., Ballester, J.L., Ramishvili, G., Shergelashvili, B., Hanslmeier, A., Poedts, S. (2016) Rieger-type periodicity during solar cycles 14–24: estimation of dynamo magnetic field strength in the solar interior. *Astrophys. J.* 826(1):55. DOI: https://doi.org/10.3847/0004-637X/826/1/55

Gurgenashvili, E., Zaqarashvili, T.V., Kukhianidze, V., Oliver, R., Ballester, J.L., Dikpati, M., McIntosh, S.W. (2017) North–South Asymmetry in Rieger-type Periodicity during Solar Cycles 19–23. *Astrophys. J.* 845(2):137-148. DOI: https://dx.doi.org/10.3847/1538-4357/aa830a

Kuznetsova, Yu.G., Pavlenko, E.P., Sharipova, L.M., Shugarov, S.Yu. (1999) Observations of Typical, Rare and Unique Phenomena in Close Binaries with Extremal Mass Ratio. *Odessa Astron. Pub.* 12:197-200. BIB: https://ui.adsabs.harvard.edu/#abs/1999OAP....12..197K

Lalitha S., Schmitt, J.H., Dash S. (2018) Atmospheric mass-loss of extrasolar planets orbiting magnetically active host stars. *Mon. Not. R. Astron. Soc.* 477(1):808–815. DOI: https://doi.org/10.1093/mnras/sty732

Lepping, R.P., Acuna, M.H., Burlaga, L.F. et al. (1995) The WIND magnetic field investigation. *Space Sci. Rev.* 71:207–229. DOI: https://doi.org/10.1007/BF00751330

Lockwood, M., Stamper, R. Wild, M. (1999) A doubling of the Sun's coronal magnetic field during the past 100 years. *Nature* 399:437–439. DOI: https://doi.org/10.1038/20867

Luhman, K.L., Adame, L., D'Alessio, P., Calvet, N., Hartmann, L., Megeath, S.T., Fazio, G.G. (2005) Discovery of a Planetary-Mass Brown Dwarf with a Circumstellar Disk. *Astrophys. J.* 635(1):L93. DOI: https://doi.org/10.1086/498868

Maehara, H., Shibayama, T., Notsu, S. et al. (2012) Superflares on solar-type stars. *Nature* 485:478–481. DOI: https://doi.org/10.1038/nature11063

Maehara, H., Shibayama, T., Notsu, Y., Notsu, S., Honda, S., Nogami, D., Shibata, K. (2015) Statistical properties of superflares on solar-type stars based on 1-min cadence data. *Earth Planet. Sp.* 67:59. DOI: https://doi.org/10.1186/s40623-015-0217-z

Von Neumann, J. (1941) Distribution of the Ratio of the Mean Square Successive Difference to the Variance. *Ann. Math. Statist.* 12(4):367-395. DOI: https://doi.org/10.1214/aoms/1177731677

Von Neumann, J. (1942) A Further Remark Concerning the Distribution of the Ratio of the Mean Square Successive Difference to the Variance. *Ann. Math. Statist.* 13(1):86-88. DOI: https://doi.org/10.1214/aoms/1177731645

Niroma, T. (2009) Understanding Solar Behaviour and its Influence on Climate. In: Natural drivers of weather and climate, Special Issue of *Energy & Environment* 20(1/2):145-159. DOI: https://doi.org/10.1260%2F095830509787689114

Omerbashich, M. (2021d) Magnetar-type bursting evolution of Jupiter global magnetoactivity since 1996. *In review*. DOI: https://doi.org/10.5281/zenodo.5508274

Omerbashich, M. (2021c) External forcing of Moon and Earth seismicity at Rieger periods. *In review*. DOI: https://doi.org/10.5281/zenodo.5069075

Omerbashich, M. (2021b) Extramartian forcing of Mars seismicity at Rieger periods. *In review*. DOI: https://doi.org/10.5281/zenodo.4921735

Omerbashich, M. (2021a) Non-marine tetrapod extinctions solve extinction periodicity mystery. *Hist. Biol.* 34 (29 March). DOI: https://doi.org/10.1080/08912963.2021.1907367

Omerbashich, M. (2009) *Method for Measuring Field Dynamics*. US Patent #20090192741, US PTO. https://worldwide.espacenet.com/publicationDetails/biblio?CC=US&NR=2009192741A1

Omerbashich, M. (2007) Magnification of mantle resonance as a cause of tectonics. *Geodinamica Acta* 20:6:369-383. DOI: https://doi.org/10.3166/ga.20.369-383

Omerbashich, M. (2006) Gauss–Vaníček Spectral Analysis of the Sepkoski Compendium: No New Life Cycles. *Comp. Sci. Eng.* 8(4):26–30. DOI: https://doi.org/10.1109/MCSE.2006.68 (Erratum due to journal error. *Comp. Sci. Eng.* 9(4):5–6. DOI: https://doi.org/10.1109/MCSE.2007.79; full text: https://arxiv.org/abs/math-ph/0608014)

Omerbashich, M. (2003) *Earth-model Discrimination Method*. Ph.D. Dissertation, pp.129. ProQuest, USA. DOI: https://doi.org/10.6084/m9.figshare.12847304

Pagiatakis, S. (1999) Stochastic significance of peaks in the least-squares spectrum. *J. Geod.* 73:67-78. DOI: https://doi.org/10.1007/s001900050220

Pettersen, B.R. (1989) A review of stellar flares and their characteristics. Sol. Phys. 121:299–312. DOI: https://doi.org/10.1007/BF00161702

Raymond, S.N., Morbidelli, M. (2022) Planet formation: key mechanisms and global models. arXiv https://arxiv.org/abs/2002.05756. In: Biazzo, K., Bozza, V., Mancini, L., Sozzetti, A. (Eds.) *Demographics of Exoplanetary Systems*. Lecture Notes of the 3rd Advanced School on Exoplanetary Science. https://www.springer.com/gp/book/9783030881238

Rieger, E., Share, G.H., Forrest, D.J., Kanbach, G., Reppin, C., Chupp, E.L. (1984) A 154-day periodicity in the occurrence of hard solar flares? *Nature* 312:623–625. DOI: https://doi.org/10.1038/312623a0

Rubenstein, E.P., Schaefer, B.E. (2000) Are Superflares on Solar Analogues Caused by Extrasolar Planets? *Astrophys. J.* 529(2):1031. DOI: https://doi.org/10.1086/308326

Schaefer, B.E., King, J.R., Deliyannis, C.P. (2000) Superflares on Ordinary Solar-Type Stars. *Astrophys. J.* 529(2):1026. DOI: https://doi.org/10.1086/308325

Scharf, C.A. (2010) Possible constraints on exoplanet magnetic field strengths from planet-star interaction. *Astrophys. J.* 722:1547–1555. DOI: http://dx.doi.org/10.1088/0004-637X/722/2/1547

Scherrer, P.H., Wilcox, J.M., Svalgaard, L., Duvall, Jr. T.L., Dittmer, P.H., Gustafson, E.K. (1977) The mean magnetic field of the Sun: Observations at Stanford. *Sol. Phys.* 54:353–361. DOI: https://doi.org/10.1007/BF00159925

Simpson, J.F. (1968) Solar activity as a triggering mechanism for earthquakes. *Earth Planet. Sci. Lett.* 3:417-425. DOI: https://doi.org/10.1016/0012-821X(67)90071-4

Taylor, J., Hamilton, S. (1972) Some tests of the Vaníček Method of spectral analysis. *Astrophys. Space Sci.* 17:357–367. DOI: https://doi.org/10.1007/BF00642907

Tsurutani, B.T., Gonzalez, W.D., Lakhina, G.S., Alex, S. (2003) The extreme magnetic storm of 1–2 September 1859. *J. Geophys. Res.* 108:1268. DOI: https://doi.org/10.1029/2002JA009504

Tu, Z.-L., Yang, M., Zhang, Z.J., Wang, F.Y. (2020) Superflares on Solar-type Stars from the First Year Observation of TESS. *Astrophys. J.* 890:46. DOI: https://doi.org/10.3847/1538-4357/ab6606

Usoskin, I.G., Gallet, Y., Lopes, F., Kovaltsov, G.A., Hulot, G. (2016) Solar activity during the Holocene: the Hallstatt cycle and its consequence for grand minima and maxima. *Astron. Astrophys.* 587:A150. DOI: http://dx.doi.org/10.1051/0004-6361/201527295

Usoskin, I.G., Solanki, S.K., Kovaltsov, G.A. (2007) Grand minima and maxima of solar activity: new observational constraints. *Astronomy & Astrophysics* 471(1):301-309. DOI: https://doi.org/10.1051/0004-6361:20077704

Vaníček, P. (1969) Approximate Spectral Analysis by Least-Squares Fit. *Astrophys. Space Sci.* 4(4):387–391. DOI: https://doi.org/10.1007/BF00651344

Vaníček, P. (1971) Further Development and Properties of the Spectral Analysis by Least-Squares Fit. *Astrophys. Space Sci.* 12(1):10–33. DOI: https://doi.org/10.1007/BF00656134

Wells, D.E., Vaníček, P., Pagiatakis, S. (1985) *Least squares spectral analysis revisited*. Department of Geodesy & Geomatics Engineering Technical Report 84, University of New Brunswick, Canada. Link: http://www2.unb.ca/gge/Pubs/TR84.pdf

Zaqarashvili, T.V., Carbonell, M., Oliver, R., Ballester, J.L. (2010) Magnetic Rossby waves in the solar tachocline and Rieger-type periodicities. *Astrophys. J.* 709(2):749–758. DOI: https://doi.org/10.1088/0004-637X/709/2/749